

Reports

Lunar Topography: First Radar-Interferometer Measurements of the Alphonsus-Ptolemaeus-Arzachel Region

Abstract. Radar interferometry is a new technique for accurately measuring the topography of the lunar surface from the earth. Measurements have been made with this technique of an area including the craters Ptolemaeus, Alphonsus, and Arzachel and a portion of Mare Nubium. There is evidence for a late episode of volcanism that partially filled two of the craters through a crustal fault of Imbrian origin. Several other features of the topography, particularly those coinciding with local gravitational anomalies, can be correlated with flow events.

The first results of a new radar-astronomy technique for the direct measurement of the topography of the lunar surface are reported here (1). A detailed knowledge of the lunar topography, when combined with measurements of the surface gravitational anomalies (mascons) (2), can yield powerful clues to the most recent thermal history of the lunar crust, and will certainly elucidate the bulk thermal history and the accretion rate (or other primordial events) on the moon. Such an analysis has already been attempted with existing information on lunar topography (3) by using photogrammetry from earth-based optical photography. In this case, however, accuracy is very difficult to obtain because of the small range of lunar libration angles ($\pm 8^\circ$ maximum) available from earth observations.

By careful selection of photographs and of features and with meticulous scaling and star-calibrating procedures, it has been possible to improve the accuracy of photogrammetry results (4). However, a precision of 1 km seems to be the limit with this technique, with 2 to 3 km being a more realistic estimate (5). An additional contribution to the uncertainty is the inherent limitation of the technique to sharp and unambiguously defined features, so that elevation contours on a smaller scale must come from interpolations over great distances between the set of measured points.

In the present work we used an extension of the earlier techniques for measuring radar backscattering properties (6). In those backscatter measurements, high resolution on the lunar surface was obtained by analyzing the

lunar echo simultaneously in both time delay and Doppler frequency. The resulting two-dimensional resolution was at least 200 times finer than the spatial resolution of the radar antenna beam itself (2 km compared with 400 km) at the lunar surface.

The extension of these techniques to a three-dimensional measurement of the lunar surface is accomplished by the use of a radio-interferometer receiver for the lunar echo signals (1, 7). For a brief explanation of the technique, refer to Fig. 1, which shows a diagram of the time and frequency resolution of the radar echo from a solid body (such as the moon) with a nonzero apparent angular rotation. Echoes received by a single radar receiver may be analyzed in both time delay and Doppler frequency shift. All echoes received at a given instant after the time of transmission of the signal originate in a known spherical surface (in a frame fixed to the radar). In addition, all echoes observed to have a given Doppler frequency shift with respect to the center of mass of the rotating moon similarly originate in a quasi-planar surface containing the radar line of sight and parallel to the Doppler axis (1). Both surfaces have a nonzero thickness corresponding to the uncertainties in the two measurements, which are functions, respectively, of the duration of the transmitted pulse and the width of the spectral bands resulting from the frequency analysis of the echo.

As shown in Fig. 1, the fundamental delay-Doppler resolution cell is the intersection of these two surfaces of finite thickness, and has a shape we call a "stick" that is closely bounded

in two dimensions and unbounded in the third. In the earlier measurements of surface reflectivity (6) the surface element was assumed to lie at the intersection of the resolved stick with a sphere 1738 km in diameter, centered on the lunar center of mass. In the present work, we use a radar interferometer to measure directly the location of the lunar surface along the stick.

Our interferometer consists of the 36-m antenna at Haystack Observatory as one element, and the 18-m Westford communications antenna, located about 1200 m to the south, as the other (8). Areas of the moon are illuminated as if for a backscatter measurement (6) by the Haystack radar at a frequency of 7840 Mhz. The echo signals are received and processed from both Haystack and Westford independently. A cable link between the two sites provides the necessary common phase reference. Separate maps of the complex backscatter are produced from each site; then the two complex signals from corresponding resolution elements on the lunar surface are cross-multiplied. The magnitude of the complex cross-product is then proportional to the strength of the backscattered signal, if perfect correlation between the two signals is assumed, and the phase locates the surface element in the fringe pattern of the interferometer. By an appropriate choice of the observing time, the geometry can be such that the fringe pattern is more or less perpendicular to the resolution stick. The difference between the measured phase and a value calculated for a perfect sphere is then proportional to the distance between the true lunar surface and that sphere, along the direction of the resolution stick.

The time and frequency resolution elements in the present experiment have projected areas of about 1 by 2 km on the lunar surface. The elevation accuracy is generally better than 500 m, and a single observation (of about 10 minutes duration) yields at one time the map of an entire area 100 by 200 km.

Figure 2 presents the results of radar measurements of the area shown in the Lunar Orbiter photograph of Fig. 3. The map covers an area about 400 km square, centered approximately at 15°S , 4°W . Included are the major craters Alphonsus (about 13°S , 2°W), Arzachel (18°S , 1.5°W), and Alpetragius (15.5°S , 4°W), as well as the southern part of Ptolemaeus (8°S , 0.5°W). A portion of Mare Nubium

appears west of the 8°W meridian and extends in a band eastward toward Alphonsus.

Several features of the surface elevation stand out on the maps and are summarized in Table 1.

1) In the Mare Nubium region, the change in elevation is less than 500 m over a distance of 100 km east to west and almost 250 km north to south. This is of interest because errors hypothesized in the measurement system might produce artificial slopes in the topography measured by radar; the absence of such slopes over Nubium supports the relative accuracy of these results, especially since our earlier measurements also show this area to be flat.

Measurements of surface height are expected to be more accurate for areas like this, which are near the central lunar meridian. When the Doppler axis is oriented in the north-south direction, as it is for such a measurement (Fig. 1), the major component in the apparent angular velocity of the moon is the well-understood rotation of the earth. Areas near the lunar equator, on the other hand, must be measured when the Doppler axis is oriented east to west, which can occur only when the earth's rotation contributes as little as possible to the apparent angular velocity, that is, near moonrise or moonset. In this case, the less certain lunar position and velocity are of primary importance in the topography calculations, and absolute results are expected to be somewhat more questionable.

2) The floors of the three large craters—Ptolemaeus, Alphonsus, and Arzachel—are level within about 500 m, except for the radial ridges and surrounding slopes in the southern half of Alphonsus and Arzachel. Such level floors are to be expected if the craters were partially filled by lava flows subsequent to their formation, as Orbiter

Table 1. Relative elevations of features in the Ptolemaeus-Alphonsus-Arzachel region.

Feature	Elevation (m)	
	Alphonsus	Arzachel
Northern level floor*	900	300
Top of southern sloping floor	1200	1200
Ridge (mean)	~1200	~1200
Central peak	1500	1500

* The elevation of the Ptolemaeus floor is 1500 m, and that of the Mare Nubium surface is approximately 1200 m.

photographs seem to indicate (Fig. 3).

Of more interest is the difference in the levels of the three craters and the comparison with the level of Mare Nubium to the west. Based on stratigraphy and on the observed erosion of wall features, the time sequence of the three events, from oldest to most recent, is Ptolemaeus, Alphonsus, and Arzachel. This is also the order of their floor elevations, with Ptolemaeus having the highest level and Arzachel the lowest; the level of Mare Nubium comes between those of Ptolemaeus and Alphonsus. If crater filling is carried out by a series of successive thin flows, as seems to be the case for the Palus Putredinus-Mare Imbrium region (6, 9), then the difference in levels may result from the cessation of major volcanic activity at a given time, before the younger craters had been filled to the level of the older ones.

This simplistic view of crater filling must be modified in light of the ridge structures mentioned above. Visible in the southern half of both Alphonsus and Arzachel (Fig. 2) is a second, shallow, higher level of fill that starts at the east-west diameter of the level part of the crater floor and slopes upward toward the southern rim. In the case of Alphonsus, the backscatter maps for 3.8-cm radar also show a small but real increase in the back-

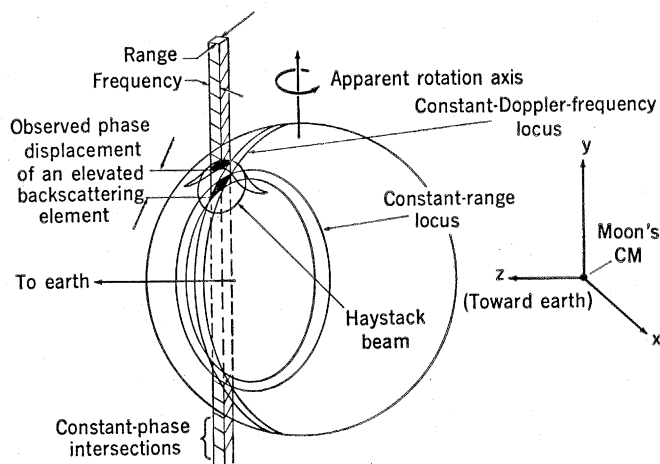
scatter from the slope with respect to the level floor that is not explainable by the small difference in slope itself. As usual with the radar data, it is not possible to distinguish between an increase in roughness and a difference in dielectric constant or electromagnetic attenuation, but it does appear that the southern and northern halves of the crater floor have different origins. Arzachel appears to show a similar difference, but there has not yet been a detailed examination of its radar backscatter map.

Centered on the sloping half of the two crater floors is a radial ridge, extending from the central peak of the crater toward the rim in a south-southeast direction. The two ridges are aligned quite well with each other and also with the well-known series of ridges and rilles radial to the Imbrium basin (10). The southwestern section of the hexagonal rim of Ptolemaeus is also on the same radius of Imbrium. Another strong argument for the common morphology of the Alphonsus ridge and the Ptolemaeus wall is the unbroken, shallow, cratered rille (Fig. 3) that runs 250 km along the Alphonsus ridge, across both crater walls, and along the western edge of Ptolemaeus' floor. This appears to be direct evidence of an Imbrian crustal fracture.

It has been suggested (11), that the ridge and sloping fill in Alphonsus are composed of ejecta from the more recent Arzachel event. An alternate, more probable explanation for the fill in the two craters would be a late flow of viscous lava through crustal faults remaining from the Imbrium impact. This is more likely because of the similar topography in Arzachel itself and the absence of a crater of similar size to the south, from which ejecta might have been deposited in Arzachel, and especially because of the remarkable orientation of the two ridges with the Imbrium basin. It is assumed that the flow material must have been viscous since a highly fluid material would presumably have overspread the crater floor, as earlier flows must have done, rather than remain piled up in the southern half of the crater.

This hypothesis of crustal faulting and subsequent upwelling of lava is supported by the topography of the two ridges. As shown in Table 1, in spite of the fact that the elevations of the level crater floors differ by about 600 m, the central peaks rise to about the same elevation datum. In the case of Alphonsus this is a height of 600 m above the crater floor, whereas in the case of

Fig. 1. Schematic resolution of a radar echo from the lunar surface in time delay and Doppler frequency. The relative cross section of the resolved element is shown about 100 times enlarged.



Arzachel it is 1200 m. If we rule out the perennial but unsatisfying explanation of coincidence, then one alternative is filling due to hydrostatic pressure from a common magma reservoir. This suggests not only a common origin for the two ridges but also a common time of occurrence.

3) Finally, one feature of the region

that may contribute to the understanding of early lunar volcanism is the negative gravitational anomaly over Ptolemaeus, measured on both the Apollo 12 and the Apollo 14 missions (12). The hypothesis was that the negative anomaly represents the material ejected from the crater during its formation, and so the negative mascon was ex-

plained by stating that any subsequent fill was insufficient to compensate for the original loss of mass. In the case of Ptolemaeus, however, its floor is above the level of Mare Nubium by 200 to 500 m even though its gravitational anomaly is apparently negative with respect to Nubium. There is still a possibility of a small local negative

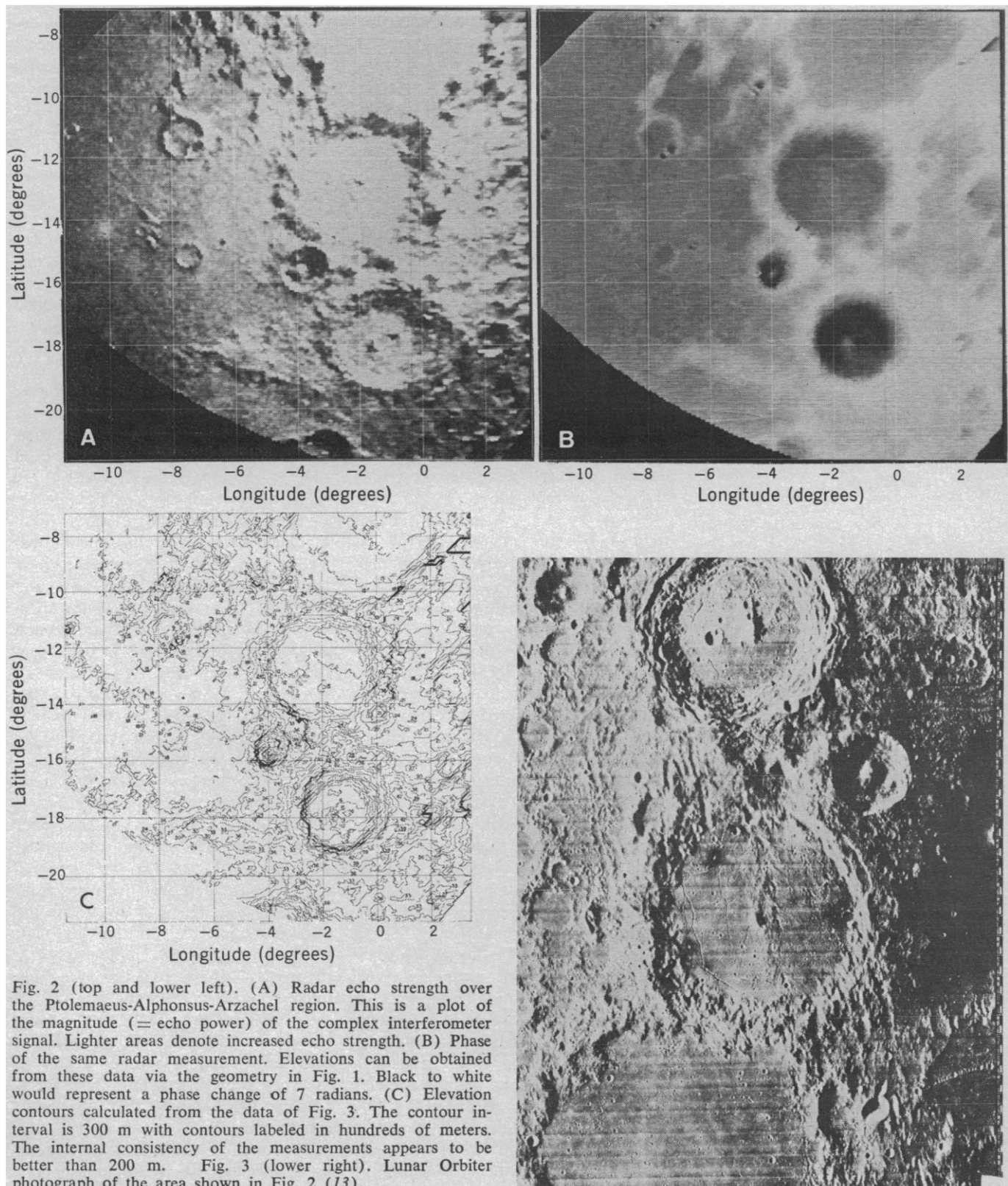


Fig. 2 (top and lower left). (A) Radar echo strength over the Ptolemaeus-Alphonsus-Arzachel region. This is a plot of the magnitude (= echo power) of the complex interferometer signal. Lighter areas denote increased echo strength. (B) Phase of the same radar measurement. Elevations can be obtained from these data via the geometry in Fig. 1. Black to white would represent a phase change of 7 radians. (C) Elevation contours calculated from the data of Fig. 3. The contour interval is 300 m with contours labeled in hundreds of meters. The internal consistency of the measurements appears to be better than 200 m. Fig. 3 (lower right). Lunar Orbiter photograph of the area shown in Fig. 2 (13).

anomaly for the western edge of Nubium, since the low-altitude orbital data for Ptolemaeus did not extend far enough south to cover Nubium also. If this is not the case, we are left with the conclusion that at least some of the material in the Ptolemaeus fill is of lower density than the Nubium flow, or that a deep layer of low-density regolith underlies the superficial Ptolemaeus flow. The hypothesis of a low-density flow and the similar elevations appear to agree with the hypothesis of a relatively recent high-viscosity flow in Alphonsus and Arzachel, comprising feldspathic or anorthositic material having a low density as a result of the great proportion of light, volatile elements. However, the high viscosity of such lava might not be compatible with the smooth, level floor observed in Ptolemaeus unless the temperature of the flow or of the neighboring lunar surface was great enough to permit the flow to reach a smooth level only in Ptolemaeus.

S. H. ZISK

Haystack Observatory,
Westford, Massachusetts 01886

References and Notes

1. A more complete discussion of the techniques is given in I. I. Shapiro, S. H. Zisk, A. E. E. Rogers, M. A. Slade, T. W. Thompson, *Science* **178**, 939 (1972).
2. P. M. Muller and W. L. Sjogren, *ibid.* **161**, 680 (1968).
3. W. M. Kaula, *Phys. Earth Planet. Interiors* **4**, 185 (1971).
4. Z. Kopal, "Scientific Report No. 2" (USAF contract F6105-2-68-C-0002, University of Manchester, Manchester, England, June 1970).
5. For references and an evaluation of earlier results see V. S. Kisilyuk, *Sov. Astron. AJ* **14**, 487 (1970).
6. S. H. Zisk, M. H. Carr, H. Masursky, R. W. Shorthill, T. W. Thompson, *Science* **173**, 808 (1971); S. H. Zisk and T. Hagfors, "Final Report" (NASA contract NAS9-7830, M.I.T. Lincoln Laboratory, Lexington, September 1970).
7. S. H. Zisk, *Moon* **4**, 296 (1972).
8. The Haystack-Westford interferometer system was originally built for mapping the radar reflectivity of Venus. See A. E. E. Rogers and R. P. Ingalls, *Radio Sci.* **5**, 425 (1970).
9. Apollo Lunar Geology Investigation Team, *Science* **175**, 407 (1972).
10. W. K. Hartmann, *Commun. Lunar Planet. Lab. No. 24* (1964).
11. See, for example, D. E. Wilhelms and J. F. McCauley, *Geological Survey Map I-703* (U.S. Geological Survey, Washington, D.C., 1971).
12. P. Gottlieb, P. M. Muller, W. L. Sjogren, W. R. Wollenhaupt, *Science* **168**, 477 (1970); W. L. Sjogren, P. Gottlieb, P. M. Muller, W. Wollenhaupt, *ibid.* **175**, 165 (1972).
13. Lunar Orbiter IV high-resolution frame 108.
14. Thanks to G. H. Pettengill and T. R. McGechin for useful and stimulating discussions, and to R. P. Ingalls, J. I. Levine, G. W. Catuna, and others at Haystack Observatory for assistance with the radar and data processing. Particular thanks are due A. E. E. Rogers for indispensable assistance with the interferometer and the original computer programs for processing the present moon topography data. This work was carried out at Haystack Observatory, which is operated by the Massachusetts Institute of Technology for the Northeast Radio Observatory Corporation. Support by NASA contract NAS9-7830 is gratefully acknowledged.

31 March 1972; revised 5 July 1972

Uptake and Binding of Uranyl Ions by Barley Roots

Abstract. *After undergoing the processing for electron microscopy, bound uranyl ions are revealed as characteristic electron-opaque crystals. Meristematic walls and associated vesicles become heavily labeled, while pinocytotic accumulation into vacuoles seems probable in cap cells and those just behind the meristem. The endodermal Casparian strip and suberized lamella are effective barriers to the passage of uranyl ions.*

When seminal barley roots 20 to 30 centimeters long were placed in dilute solutions of uranyl acetate and then processed for electron microscopy (1), typical electron-opaque crystals were found in cell walls and, sometimes, within cells. These crystals are thought to be a uranyl complex resulting, at least in part, from the reaction of bound uranyl ions with phosphate in the buffered fixative solutions (2). There is no doubt that the electron-opacity is caused by the presence of uranium: omission of osmium tetroxide fixation does not affect the appearance of the crystals (2); the crystals are quite characteristic and easily recognizable in the electron microscope; and they are present regardless of the presence or absence of any post-staining procedure. We have used this system as part of a program to investigate the uptake and binding of electron-opaque markers at different points along barley roots (3).

Uranyl acetate was used in concentrations of $10^{-3}M$ or $10^{-4}M$ in aqueous solution; $10^{-3}M$ uranyl acetate is relatively toxic and exposure periods were kept below 1 hour. Electron-opaque crystals were only found in the exterior three to four layers of cortical cells, and therefore this concentration was not used further. No toxic effects were noted in roots grown for almost 1 day in $10^{-4}M$ solution, and this concentration was used for all subsequent experiments.

The apical 2 millimeters of a barley root include both root cap and meristematic zone. Our observations in the root cap generally supported those of Wheeler and Hanchey (2), although crystals were only seen in cytoplasmic vesicles relatively infrequently. Some walls contained much higher densities of crystals than others, peripheral walls usually being less heavily labeled. In the meristematic zone itself the presence of uranyl crystals led to extremely high opacity of many walls (Fig. 1A) although, once again, there were distinct gradations of density (Fig. 1B). Newly formed walls, even cell plates, and closely associated vesicles were the most heavily labeled of all (Fig. 1C).

The region immediately behind the meristematic zone is characterized by cells which are expanding. The endodermis is now well formed and recognizable, although the Casparian strip does not become easily recognizable until 5 to 7 mm from the tip. The cortical cells in this region 2 to 3 mm from the tip had dilated plasmalemma membranes, forming cavities between themselves and the cell wall, which were filled with crystals (Fig. 1D). Crystals were also present in vacuoles, including the vacuoles of endodermal cells (Fig. 1E). The radial walls of endodermal cells generally presented no barrier to centripetal penetration.

As soon as the Casparian strip is laid down (5 to 7 mm behind the root tip), penetration of the tracer solution beyond the outer tangential wall of the endodermal cell and the outer parts of the radial walls is completely blocked (Fig. 1, F and G). The cortical cell walls were relatively heavily labeled, as were the intercellular spaces. By 8 to 12 cm from the tip, the endodermal walls have started to undergo their typical thickening of the inner and radial sides. In some cases quite thick walled endodermal cells are found adjacent to those only possessing a Casparian strip (Fig. 1, H and J). Once again the Casparian strip is the barrier to passage of the marker inward through the cell wall, but the deposition of the "suberized lamella," prior to further wall thickening completely precludes any further access of the marker solution to the inner edge of any part of the endodermal wall (Fig. 1, H and I).

The results described here are from experiments designed to investigate the uptake of molecules and ions by plant roots. The first few millimeters are, therefore, of comparatively little interest in this connection, although the observations made have some importance. Just behind the meristematic zone, and to a lesser degree in the root cap, micrographs have been obtained which suggest that pinocytotic activity may be taking place. On the other hand, in the meristematic zone itself the observations would generally